Phosphorylation-mediated regulation of the Bacillus anthracis phosphoglycerate mutase by the Ser/Thr protein kinase PrkC

Richa Virmani, Prashant Pradhan, Jayadev Joshi, Avril Luyang Wang, Hem Chandra Joshi, Andaleeb Sajid, Anoop Singh, Vishal Sharma, Bishwajit Kundu, Daniel Blankenberg, et al.

Phosphorylation-mediated regulation of the *Bacillus anthracis* phosphoglycerate mutase by the Ser/Thr protein kinase PrkC
Running title: Threonine Phosphorylation mediated regulation of Pgm

Richa Virmani[1], Prashant Pradhan[2], Jayadev Joshi[3], Avril Luyang Wang[4], Hem Chandra Joshi[1], Andaleeb Sajid[5], Anoop Singh[1], Vishal Sharma[1], Bishwajit Kundu[2], Daniel Blankenberg[3], Virginie Molle[6], Yogendra Singh[1,]* and Gunjan Arora[5,]*

[1] Department of Zoology, University of Delhi, Delhi 110007, India.
[2] Kusuma School of Biological Sciences, IIT Delhi, Hauz Khas, New Delhi 110016, India.
[3] Genomic Medicine Institute, Lerner Research Institute, Cleveland Clinic, Cleveland, OH, 44195, USA.
[4] Department of Molecular Genetics and Microbiology, University of Toronto, Toronto, M5S1A8, Canada.
[5] Department of Internal Medicine, Yale University School of Medicine, New Haven, Connecticut 06520, USA.
[6] Laboratory of Pathogen Host Interactions, Université de Montpellier, CNRS, UMR 5235, Montpellier, France.

*Corresponding Author:

Yogendra Singh, Department of Zoology, University of Delhi, Delhi 110007, India. Email: ysinghdu@gmail.com

Gunjan Arora, Department of Internal Medicine, Yale University School of Medicine, New Haven, Connecticut 06520, USA. Email: arorag1983@gmail.com

Keywords: Phosphoglycerate mutase, Glycolysis, *Bacillus anthracis*, Phosphorylation, Signaling

Abstract

Bacillus anthracis Ser/Thr protein kinase PrkC is necessary for phenotypic memory and spore germination, and the loss of PrkC-dependent phosphorylation events affect the spore development. During sporulation, *Bacillus sp.* can store 3-Phosphoglycerate (3-PGA) that will be required at the onset of germination when ATP will be necessary. The Phosphoglycerate mutase (Pgm) catalyzes the isomerization of 2-PGA and 3-PGA and is important for spore germination as a key metabolic enzyme that maintains 3-PGA pool at later events. Therefore, regulation of Pgm is important for an efficient spore germination process and metabolic switching. While the increased expression of Pgm in *B. anthracis* decreases spore germination efficiency, it remains unexplored if PrkC could directly influence Pgm activity. Here, we report the phosphorylation and regulation of Pgm by PrkC and its impact on Pgm stability and catalytic activity. Mass spectrometry revealed Pgm phosphorylation on seven threonine residues. *In silico* mutational analysis highlighted the role of Thr[459] residue towards metal and substrate binding. Altogether, we demonstrated that PrkC-mediated Pgm phosphorylation negatively regulates its activity that is essential to maintain Pgm in its apo-like isoform before germination. This study advances the role of Pgm regulation that represents an important switch for *B. anthracis* resumption of metabolism and spore germination.

Keywords: Metabolism, Phosphoglycerate mutase, Phosphorylation, Ser/Thr Protein Kinase, Spore germination

INTRODUCTION

Bacillus anthracis is an obligate human pathogen generating life-threatening cutaneous, gastrointestinal or pulmonary infections after contact with infected animals [1,2]. This pathogen is known for its remarkable ability to form spores and capacity to survive for extended periods of time in the environment. During the course of host infection, spores germinate and grow out as vegetative bacilli producing toxins and virulence factors [3,4]. Deciphering spore germination processes is a major area of research in bacteriology. The prerequisite for germination is to upstart the metabolism processes with the scarce resources available in the spore. Then, glycolysis is the first metabolic step to generate energy and it involves several metabolites and intermediates. For instance, 3-Phosphoglycerate (3-PGA) is the only known stable metabolite present in spores despite the presence of its catabolic/hydrolyzing enzymes. *Bacillus* sp. are known to store sufficient levels of 3-PGA depot during sporulation that will be required during germination [5-7]. The 2,3-biphosphoglycerate- independent phosphoglycerate mutase (Pgm) catalyzes the reversible hydrolysis of 3-PGA to 2-PGA and represents a key metabolic enzyme involved in 3-PGA metabolite pool accumulation in spores. The inactivity of Pgm during sporulation and its rapid activation for 3-PGA hydrolysis at the onset of germination requires a tight regulation that is critical for an efficient spore germination process [5,8].

Previous studies confirmed the importance of Pgm in *Bacillus* spores, where its absence makes the *Bacillus subtilis* strain asporogenous [9], while its overexpression in *B. anthracis* decreases spore germination efficiency [10]. In *Bacillus* sp., the role of the Ser/Thr protein kinase PrkC in sporulation and germination events is well established [10-14]. In fact, we previously showed that the PrkC-mediated phosphorylation of Eno was critical for phenotypic memory and spore germination in *B. anthracis* [10]. Phenotypic memory corresponds to the persistence of vegetative components into the spore that will be required for proper germination [10,15-18].

Interestingly, *B. subtilis* phosphoproteome studies identified Pgm as a phosphorylated protein [19,20]. Therefore, we hypothesized that Pgm could be regulated by phosphorylation via *B. anthracis* kinases like PrkC. Additionally, in order to explore the structural basis of Pgm phosphorylation and signaling, we generated *in-silico* phosphoablative and phosphomimetic mutants bound to 3-PGA and Mn^{2+}. Our structural investigations combined with biochemical analysis revealed the mechanistic insights of Pgm activation and inhibition, thus highlighting the mechanisms underlying 3-PGA accumulation and metabolic resumption in spores.

MATERIALS AND METHODS

Bacterial strains, and cloning and expression of B. anthracis genes
The *E. coli* (DH5α and BL21(DE3)) and *B. anthracis* Sterne strains (wild type *Bas*-wt and *BasΔprkC* [11] were grown and maintained as described before [21]. The genes encoding *prkC* (catalytic domain (PrkCc), Bas3713), *prkD* (Bas2152) and *prkG* (Bas2037) were cloned as described previously [22,23]. The details of primers and plasmids are provided in Table 1. *B. anthracis* Pgm encoding gene (Bas4986, 1-509 aa) was cloned into pPRO-Ex-Htc plasmid. The recombinant clones were confirmed with DNA sequencing (SciGenome).

B. anthracis Pgm protein was overexpressed and purified in *E. coli* as described before [10,21]. The *pgm* gene Bas4986 was co-transformed with pACYC PrkC or pACYC PrpC [10]. For Pgm polyclonal antibody generation, the purified protein was used to immunize BALB/c mice as described before (n=3) (Animal House Delhi University, Delhi) [10]. Immune sera was tested for specificity and titrated by immunoblotting. Standard protocols for immunoblotting were followed as described earlier [24,25]. The antibodies and dilutions used anti-Pgm antibody 1:20,000 dilution. Two-dimensional gel electrophoresis was performed as described earlier [21,24,25].

Mass spectrometry
Sliced gel pieces were trypsinized and the peptides separated were analyzed as described earlier [26].

In vitro kinase assay
PrkCc, PrkD and PrkG (0.5-0.8 μg) were used to phosphorylate Pgm (2-5 μg) [23]. Proteins were resolved by SDS-PAGE and analyzed.

Phosphoglycerate mutase activity assay

The activities of Pgm-UP and Pgm-P (0.5 μg) were measured using the Phosphoglycerate mutase fluorometric/colorimetric activity assay kit as per manufacturer′s protocol (Biovision).

Manganese binding assay

The purified proteins were titrated with or without 10 μM 3-PGA (Sigma) with $MnCl_2$ (0.5 mM). The emission spectra were recorded from 300 nm to 430 nm after excitation at 280 nm (Fluoromax-3 spectrofluorometer; Jobin Yvon Horiba) with an integration time of 1 s [10,25].

Structure modelling and validation

Modeller 9v.24 was used to perform homology modelling of the wild-type Pgm structure using crystal structures obtained from RCSB as templates (PDB ID: 2IFY, 1EJJ, 1EQJ, 1O98, 1O99) [5,6,27,28]. Mutants (T19A, T95A, T166A, T420A, T459A, T489A, T492A) and phosphorylated wild-type structures (T459 Phosphorylated) were generated using the BuildModel module of FoldX software suite and undergo further refinement [29,30].

Docking

Molecular docking was performed using AutoDock Vina [31,32] while receptor and ligand preparation was completed using AutoDockTools 4 [33]. The ligands were obtained from reference bound structures of Pgm [5,28]. The intermediate glycerate was constructed by manually removing the phosphate group from the 2-PGA structure in Avogadro and the geometry of the resulting structure was optimized using the UFF forcefield [34]. The bound structures were analyzed using K_{DEEP} to obtain protein-ligand affinity [35].

Binding site interaction analysis

Structures that demonstrated perturbed binding affinity (T459A) underwent binding site interaction analysis using the Arpeggio webserver [36]. Bond lengths were measured using PyMOL [28]. The effects of mutations and phosphorylation on the coordination of the Mn^{2+} ions were evaluated using metal-ion docking in K_{DEEP}.

Circular dichroism spectroscopy

Conformational changes in the secondary structure of protein were monitored using J-815 CD spectropolarimeter [37].

Differential scanning calorimeter

The thermostability of Pgm proteins was measured using a MicroCal PEAQ-DSC system using 12.5 μM protein. Enthalpy change (ΔHcal) was measured as the area under the curve of the excess molar heat capacity (Cp, baseline corrected) of each transition [51].

Evolutionary conservation

To estimate the evolutionary conservation of amino acid positions in Pgm protein molecules, we aligned amino acid sequences of Pgm from 220 *Bacillus* sp. (Supplementary table S1) using MAFFT V.7.450 software [38]. This multiple sequence alignment was used as an input to the ConSurf Server [39] (http://consurf.tau.ac.il/index_proteins.php) using *B. anthracis* Pgm (PDB-2IFY) as a reference structure with default parameters. For sequence alignment, the Pgm sequences from *B. anthracis* (Uniport ID Bas; Q81X7) and *B. subtilis* (Bsu; P39773) were aligned using Clustal omega version 1.2.1.

RESULTS AND DISCUSSION

Pgm is phosphorylated in B. anthracis

The regulation of Pgm is important for 3-PGA accumulation in dormant spores and for energy needs in germinating spores. Our previous study revealed the role of PrkC in spore germination [10]. Also, a *B. subtilis* phosphoproteome study identified Pgm phosphorylation [20]. Therefore, based on Pgm homology in both species (~78% protein sequence identity, Supplementary Figure S1), we investigated

the phosphorylation status of Pgm in *B. anthracis* by using Bas-wt and BasΔprkC strains. Whole-cell protein extracts of Bas-wt and BasΔprkC were subjected to 2-D gel electrophoresis followed by immunoblotting with mouse anti-Pgm antibodies. In Bas-wt, four Pgm isoforms were identified, whereas only two Pgm isoforms were observed in BasΔprkC cells (Figure 1A and 1B). Of the four identified isoforms in Bas-wt, two were present at a pI similar to that in BasΔprkC strain, while the remaining two migrated at a higher acidic pI range (towards 3.0, Figure 1A). The expression levels of Pgm in both the strains was found to be similar (Supplementary Figure S2). Therefore, our data confirms that PrkC influences the phosphorylation status of Pgm in *B. anthracis.*

Pgm is phosphorylated by PrkC
In order to determine if PrkC can phosphorylate Pgm, we performed *in vitro* phosphorylation assay with the catalytic domain of PrkC (PrkCc) [23]. As shown in figure 1C, Pgm was phosphorylated by PrkCc. Moreover, reversibility of Pgm phosphorylation was confirmed *in vivo* in the *E. coli* surrogate host where Pgm was either co-expressed with PrkCc or with PrpC phosphatase, respectively. The purified Pgm proteins were subjected to phosphorylation-specific ProQ diamond staining (Figure 1D). Pgm was found to be phosphorylated when co-expressed with PrkCc (phosphorylated Pgm; Pgm-P), while no phosphorylation could be detected in Pgm co-expressed with PrpC (unphosphorylated Pgm; Pgm-UP). Therefore, these results demonstrate that the kinase-phosphatase pair PrkC-PrpC regulates Pgm phosphorylation reversibly.

To further validate Pgm phosphorylation, purified Pgm-P and Pgm-UP proteins were subjected to immunoblotting using anti-pThr antibodies. pThr-specific antibodies recognized Pgm-P, whereas no phosphorylation was observed on Pgm-UP (Figure 1E), thus validating the reversible phosphorylation of Pgm. Interestingly, previous phosphoproteome studies in *B. subtilis* indicated that Pgm was phosphorylated only on serine residues [20], while our result indicates that *B. anthracis* PrkC can phosphorylate Pgm on threonine residues. Before investigating the phosphorylated Pgm residues by mass spectrometry, we first analyzed the stoichiometry of purified Pgm-P and Pgm-UP proteins by 2-D gel electrophoresis followed by immunoblotting (Figure 1F). Multiple isoforms were detected for Pgm-P as compared to Pgm-UP, indicating that Pgm is phosphorylated on multiple residues.

Pgm is phosphorylated by the dual specificity protein kinases, PrkD and PrkG
PrkC is a membrane associated sensor kinase that responds to extracellular signals and mediates spore germination processes in *B. anthracis* [11,40]. Our previous study revealed the presence of the dual specificity protein kinases (DSPKs), PrkD and PrkG in *B. anthracis* [23]. Since Pgm is highly conserved and regulated, it is presumed that in the absence or inactive state of PrkC, the key phosphorylation events could be performed by PrkD and PrkG. Therefore, to check whether Pgm could represent a substrate for the two DSPKs, *in vitro* kinase assays were performed. As shown in Figure 2, Pgm was found to be phosphorylated by PrkD (Figure 2A) and PrkG (Figure 2B), respectively. Thus, we show that while Pgm is predominantly phosphorylated by PrkC, it can get phosphorylated by PrkD and PrkG dual kinases. These results are in agreement with presence of multiple isoforms of Pgm in Bas-wt and BasΔprkC strains (Figure 1A and 1F), that may correspond to DSPKs-mediated phosphorylation. Therefore, multiple protein kinases seem to play a similar role in the regulation of the Pgm enzyme in *B. anthracis*.

Pgm is phosphorylated on threonine residues
Once we identified Pgm phosphorylation, we sought to identify the specific residues modified by phosphorylation. Thus, purified Pgm-P and Pgm-UP proteins were subjected to mass spectrometry. While no phosphorylated residues were detected in Pgm-UP, we found seven phosphorylated threonine residues in Pgm-P, corresponding to Thr[19], Thr[95], Thr[166], Thr[420], Thr[459], Thr[489] and Thr[492] (Figure 2C). Interestingly, the Ser[61] phosphorylation was previously identified during the catalysis of 3-PGA and 2-PGA by the transfer of a phosphate from the glycerate to the Ser[61] residue [5,20,41], but this is the first time we report threonine phosphorylation on Pgm, which might play a role in protein activity.

Pgm catalytic activity and stability of Pgm: MnCl$_2$ complex is regulated by phosphorylation
Pgm catalyzes the reversible conversion of 3-PGA to 2-PGA [42]. To determine the effect of phosphorylation on the catalytic activity of Pgm, we performed a fluorescence/colorimetric activity

assay. This assay measures the intermediate product formed during the catalytic conversion of 3-PGA to 2-PGA and showed that Pgm-P was 40% less active than Pgm-UP (Figure 3A). This result suggests that phosphorylation negatively regulates Pgm catalytic activity.

Pgm is a metalloenzyme that absolutely and specifically requires Mn^{2+} as a cofactor for isomerization of 3-PGA to 2-PGA [5,43,44], and its activity is then highly dependent on the presence of free Mn^{2+} in spores [45]. Therefore, we decided to investigate the role of PrkC-mediated phosphorylation in the complex association of Pgm with its substrate (3-PGA) and metal cofactor (Mn^{2+}). First, we analyzed the structural arrangement of Pgm-P and Pgm-UP by CD spectroscopy. Interestingly, both isoforms showed significant differences in their secondary structure content (Supplementary Figure S3). Pgm-P displays higher helical and beta content with lower random content (Figure S3B), making it more rigid and organized in comparison to Pgm-UP whose higher random organization leads to increased flexibility and probable active conformation (Figure S3C). This difference in the structural content could be attributed to the differences in phosphorylation status. To test the stability of the protein upon substrate/cofactor addition, we used the Tryptophan (Trp) fluorescence analysis [25,46-49]. The behavior of the two Trp residues present in each isoform was analyzed to identify conformational changes in the local environment of Trp upon $MnCl_2$/3-PGA addition. As shown in Figure 3B, higher fluorescence of Pgm-UP: Mn^{2+} showed a more hydrophobic localization of Trp residue, and thus a more active conformation upon metal/substrate addition, whereas addition of substrate or $MnCl_2$ had no effect on the fluorescence intensity of Pgm-P. Therefore, the unphosphorylated Pgm-UP isoform shows more structural rearrangement and flexibility upon metal addition in comparison to the Pgm-P phosphorylated isoform, as expected from our CD data.

Higher structural stability should lead to high thermal transition midpoint (Tm) and enthalpy of unfolding [50,51]. To verify this hypothesis, differential scanning calorimetry (DSC) was performed to calculate the difference in Tm and enthalpy (ΔH) of unfolding for Pgm-P and Pgm-UP. During thermal denaturation, both isoforms displayed two states unfolding. The data revealed that Pgm-UP had a greater Tm and ΔH (Tm = 49.02 °C, ΔH=143.23±1.82 Kcal/mol) in comparison to Pgm-P (Tm = 42.24 °C, ΔH=119.43±1.02 Kcal/mol) (Figure 3C). Overall, a higher amount of energy is required to unfold the native state of Pgm-UP thus indicating a higher proportion of folded domains in Pgm-UP as compared to Pgm-P.

Effect of phosphorylation on the structure and function of Pgm

To assess the role of the different phosphorylated residues, we generated a Pgm homology model with the 3-PGA and 2-PGA ligands, based on crystal structures obtained from RCSB as templates. The structures of Pgm and its mutant derivatives were generated for *B. anthracis* and *Bacillus stearothermophilus* and the phosphorylated residues were mapped [5,6,27,28]. The ligand 2-PGA/3-PGA is bound in the protein catalytic site forming substrate-metal complex and is stabilized in the binding pocket through different polar interactions between the ligand and amino acids- Ser[61], His[122], Arg[152], Arg[184], Arg[190], Arg[260], Arg[263], His[406], and His[461] (Figure 4A). Among the seven Thr phosphorylated residues, Thr[459] was located inside the substrate/Mn^{2+}-binding pocket of the protein, while the remaining residues were located on the outer surface (Figure 2C). Domain conservation analysis indicated the conserved nature of Thr[459] amongst 220 *Bacillus* sp. which indicates the importance of this residue (Fig 4B, Supplementary Table S1).

To determine the role of the phosphorylation on these sites, we generated *in-silico* phospho-ablative Thr→Ala mutants of all the phosphorylated residues, and compared their docked structures to the wild-type for their affinity towards Mn^{2+} and their ligand 3-PGA/2-PGA. Our docking studies revealed that of all the residues tested, T459A mutant structures exhibited maximum perturbations in ligand binding affinity, thus confirming the importance of the phosphorylation in Pgm activity. Our *in-silico* analysis confirms that Thr[459] is a key residue contributing to the network of hydrogen bonds involved in stabilizing the connection between the transferase and the phosphatase domains of Pgm. Thr[459] is part of a conserved motif including the Mn^{2+} binding-His[461] residue [5] (Figure 4B and S4). Mutating Thr[459] to Ala alters the hydrophobicity of the residue thus affecting the overall hydrogen bond formation of Thr[459] as illustrated in Figure 5. Moreover, during energy minimization of the *in-silico* generated phosphoablative T459A mutant protein, we observed that the nearby residue Asp[443] undergoes a bond rotation such that the distance between OD1 and Mn^{2+} extends from a length of 2.15-2.21Å to around 3Å. Such an increase in the distance prompts the Mn^{2+} to coordinate with a much closer

OD2 of Asp[443], which is only 1.87-1.89 Å away. Thr[459] seems to influence the conformation of Asp[443] through its role in orienting a hairpin motif containing Asp[443] towards the Mn^{2+} ions [5]. Such re-orientation alters the domain-cleft and conformation of the catalytic site due to Thr to Ala mutation, leading to a decrease in 3-PGA binding affinity and distorted Mn^{2+} ion coordination (Figure 5 and Supplementary Figure S4). A similar effect was detected in the *in-silico* generated phosphorylated Thr[459] ligand complex where Thr[459]-P mutant showed altered Mn^{2+} ion coordination and allows it to preferably coordinate with OD2 of Asp[443]. Thus, any change by mutation or phosphorylation of the Thr[459] residue induces a similar negative effect on the Mn^{2+}-binding cavity. Overall, our analysis suggested that such phosphorylated residues represent critical regulators of Pgm activity and supports our result showing that unphosphorylated Pgm is more active than phosphorylated one.

Conclusion and Perspectives

The recent concept of phenotypic and plasticity memory has broadened our understanding of bacterial adaptation and behavioral changes [10,17,52]. Phenotypic plasticity allows bacteria to adapt to new environments without changing their genetic makeup. Thus, the extracellular nutritional deficiency could trigger the bacterial memory response. The cofactor independent Pgm is one such enzyme that is essential for *B. anthracis* spore germination. The eukaryotic-like Ser/Thr protein kinases in *Bacillus* sense the random fluctuations in the bacterial environment and induce temporal changes inside the bacteria which are correlated to its past memory [10,17,52,53]. In our study, we demonstrated that the Ser/Thr protein kinase PrkC phosphorylates Pgm on Thr residues and decreases its catalytic activity. We therefore propose Pgm as a major component of the phenotypic memory whose presence and phosphorylation-mediated regulation is necessary for *B. anthracis* to withstand starvation.

Author Contributions: RV and GA conceived and designed the experiments. RV, GA, PP, JJ, AW, HCJ, VS performed the experiments. RV, GA, JJ, AS, VM wrote the manuscript. VM, DB, BK, YS, GA contributed reagents and analysis tools. All authors have read and approved the manuscript.

Conflict of interest: The authors declare that they have no conflicts of interest with the contents of this article.

TABLES

Table 1. Strains, Plasmids and Primers used in this study

Gene	Vector	Restriction Site	Primers (5′→3′)	Reference
pgm (bas4986)	pProEx-HTc	FP-BamHI	GTTCTTAGGTCTTCTG<u>GGATCC</u>GTAAAATGAGAAAG	This Study
		RP-XhoI	CTCTCCTTTTTAT<u>CTCGAG</u>CAAATTATTTAATAATTG	
Duet-prkC	pACYC Duet-1	FP-NdeI	GGGTTCGACAAACGAAAG<u>CATATG</u>AAGTGCAACGTGCTG	[21]
		RP-XhoI	CTCTAGAAAGAAA<u>CTCGAG</u>TGTATTCTTCTTGTGTTGG	
prkCc (bas3713, 1-1011 bp), kinase domain	pProEx-HTc	FP-BamHI	TAGGTGAAGT<u>GGATCC</u>TGCTGATTGGAAAACGC	[23]
		RP-XhoI	TGTAATTAAAAT<u>CTCGAG</u>TCATTTATTACTTCGTTTG	
PrkD (bas2152), Full length	pProEx-HTc	FP-BamHI	GCCGTAGCTTCTTTTCA<u>GGATCC</u>TGATGAAATGGC	[23]
		RP-XhoI	GCATTACCAATACCCC<u>CTCGAG</u>CTAAAAACTTTTGAAACATC	
PrkG (bas2037) Full length	pProEx-HTc	FP-BamHI	ACGAGAGTAAGGGATCCAAATG<u>GGATCC</u>GACCAG	[23]
		RP-XhoI	GCTTTTGCATTTAAAAT<u>CTCGAG</u>ATCTATATCAG	
eno (bas4985)	pProEx-HTc	FP-BamHI	CTTATATAAAAAGGAGA<u>GGATCC</u>TTATGTCAACAATTATTGATG	[10]
		RP-XhoI	CAGTCGATTTTTTT<u>CTCGAG</u>ATAATTATCGTTTGATGTTATAAAAAG	

[a]restriction sites have been underlined

References

[1] G. Arora, R. Misra, A. Sajid, Model Systems for Pulmonary Infectious Diseases: Paradigms of Anthrax and Tuberculosis, Curr Top Med Chem 17 (2017) 2077-2099. 10.2174/1568026617666170130111324.

[2] M. Moayeri, S.H. Leppla, C. Vrentas, A.P. Pomerantsev, S. Liu, Anthrax Pathogenesis, Annu Rev Microbiol 69 (2015) 185-208. 10.1146/annurev-micro-091014-104523.

[3] M.C. Swick, T.M. Koehler, A. Driks, Surviving Between Hosts: Sporulation and Transmission, Microbiol Spectr 4 (2016). 10.1128/microbiolspec.VMBF-0029-2015.

[4] G. Christie, P. Setlow, Bacillus spore germination: Knowns, unknowns and what we need to learn, Cell Signal 74 (2020) 109729. 10.1016/j.cellsig.2020.109729.

[5] M.J. Jedrzejas, M. Chander, P. Setlow, G. Krishnasamy, Structure and mechanism of action of a novel phosphoglycerate mutase from Bacillus stearothermophilus, EMBO J 19 (2000) 1419-1431. 10.1093/emboj/19.7.1419.

[6] M. Nukui, L.V. Mello, J.E. Littlejohn, B. Setlow, P. Setlow, K. Kim, T. Leighton, M.J. Jedrzejas, Structure and molecular mechanism of Bacillus anthracis cofactor-independent phosphoglycerate mutase: a crucial enzyme for spores and growing cells of Bacillus species, Biophys J 92 (2007) 977-988. 10.1529/biophysj.106.093872.

[7] R.P. Singh, P. Setlow, Regulation of phosphoglycerate phosphomutase in developing forespores and dormant and germinated spores of Bacillus megaterium by the level of free manganous ions, J Bacteriol 139 (1979) 889-898. 10.1128/jb.139.3.889-898.1979.

[8] J. Dworkin, I.M. Shah, Exit from dormancy in microbial organisms, Nat Rev Microbiol 8 (2010) 890-896. 10.1038/nrmicro2453.

[9] M.A. Leyva-Vazquez, P. Setlow, Cloning and nucleotide sequences of the genes encoding triose phosphate isomerase, phosphoglycerate mutase, and enolase from Bacillus subtilis, J Bacteriol 176 (1994) 3903-3910. 10.1128/jb.176.13.3903-3910.1994.

[10] R. Virmani, A. Sajid, A. Singhal, M. Gaur, J. Joshi, A. Bothra, R. Garg, R. Misra, V.P. Singh, V. Molle, A.K. Goel, A. Singh, V.C. Kalia, J.K. Lee, Y. Hasija, G. Arora, Y. Singh, The Ser/Thr protein kinase PrkC imprints phenotypic memory in Bacillus anthracis spores by phosphorylating the glycolytic enzyme enolase, J Biol Chem 294 (2019) 8930-8941. 10.1074/jbc.RA118.005424.

[11] I.M. Shah, M.H. Laaberki, D.L. Popham, J. Dworkin, A eukaryotic-like Ser/Thr kinase signals bacteria to exit dormancy in response to peptidoglycan fragments, Cell 135 (2008) 486-496. 10.1016/j.cell.2008.08.039.

[12] P. Setlow, Germination of spores of Bacillus species: what we know and do not know, J Bacteriol 196 (2014) 1297-1305. 10.1128/JB.01455-13.

[13] P. Setlow, Dormant spores receive an unexpected wake-up call, Cell 135 (2008) 410-412. 10.1016/j.cell.2008.10.006.

[14] E. Madec, A. Laszkiewicz, A. Iwanicki, M. Obuchowski, S. Seror, Characterization of a membrane-linked Ser/Thr protein kinase in Bacillus subtilis, implicated in developmental processes, Mol Microbiol 46 (2002) 571-586. 10.1046/j.1365-2958.2002.03178.x.

[15] C.P. Schwall, T.E. Loman, B.M.C. Martins, S. Cortijo, C. Villava, V. Kusmartsev, T. Livesey, T. Saez, J.C.W. Locke, Tunable phenotypic variability through an autoregulatory alternative sigma factor circuit, Mol Syst Biol 17 (2021) e9832. 10.15252/msb.20209832.

[16] L. Riber, L.H. Hansen, Epigenetic Memories: The Hidden Drivers of Bacterial Persistence?, Trends Microbiol 29 (2021) 190-194. 10.1016/j.tim.2020.12.005.

[17] A. Mutlu, S. Trauth, M. Ziesack, K. Nagler, J.P. Bergeest, K. Rohr, N. Becker, T. Hofer, I.B. Bischofs, Phenotypic memory in Bacillus subtilis links dormancy entry and exit by a spore quantity-quality tradeoff, Nat Commun 9 (2018) 69. 10.1038/s41467-017-02477-1.

[18] C.S. Gokhale, S. Giaimo, P. Remigi, Memory shapes microbial populations, PLoS Comput Biol 17 (2021) e1009431. 10.1371/journal.pcbi.1009431.

[19] A. Schmidt, D.B. Trentini, S. Spiess, J. Fuhrmann, G. Ammerer, K. Mechtler, T. Clausen, Quantitative phosphoproteomics reveals the role of protein arginine phosphorylation in the bacterial stress response, Mol Cell Proteomics 13 (2014) 537-550. 10.1074/mcp.M113.032292.

[20] B. Macek, I. Mijakovic, J.V. Olsen, F. Gnad, C. Kumar, P.R. Jensen, M. Mann, The serine/threonine/tyrosine phosphoproteome of the model bacterium Bacillus subtilis, Mol Cell Proteomics 6 (2007) 697-707. 10.1074/mcp.M600464-MCP200.

[21] G. Arora, A. Sajid, R. Virmani, A. Singhal, C.M.S. Kumar, N. Dhasmana, T. Khanna, A. Maji, R. Misra, V. Molle, D. Becher, U. Gerth, S.C. Mande, Y. Singh, Ser/Thr protein kinase PrkC-mediated regulation of GroEL is critical for biofilm formation in Bacillus anthracis, NPJ Biofilms Microbiomes 3 (2017) 7. 10.1038/s41522-017-0015-4.

[22] G. Arora, A. Sajid, M.D. Arulanandh, R. Misra, A. Singhal, S. Kumar, L.K. Singh, A.R. Mattoo, R. Raj, S. Maiti, S. Basu-Modak, Y. Singh, Zinc regulates the activity of kinase-phosphatase pair (BasPrkC/BasPrpC) in Bacillus anthracis, Biometals 26 (2013) 715-730. 10.1007/s10534-013-9646-y.

[23] G. Arora, A. Sajid, M.D. Arulanandh, A. Singhal, A.R. Mattoo, A.P. Pomerantsev, S.H. Leppla, S. Maiti, Y. Singh, Unveiling the novel dual specificity protein kinases in Bacillus anthracis: identification of the first prokaryotic dual specificity tyrosine phosphorylation-regulated kinase (DYRK)-like kinase, J Biol Chem 287 (2012) 26749-26763. 10.1074/jbc.M112.351304.

[24] A. Singhal, G. Arora, A. Sajid, A. Maji, A. Bhat, R. Virmani, S. Upadhyay, V.K. Nandicoori, S. Sengupta, Y. Singh, Regulation of homocysteine metabolism by Mycobacterium tuberculosis S-adenosylhomocysteine hydrolase, Sci Rep 3 (2013) 2264. 10.1038/srep02264.

[25] A. Sajid, G. Arora, M. Gupta, A. Singhal, K. Chakraborty, V.K. Nandicoori, Y. Singh, Interaction of Mycobacterium tuberculosis elongation factor Tu with GTP is regulated by phosphorylation, J Bacteriol 193 (2011) 5347-5358. 10.1128/JB.05469-11.

[26] S.R. Schmidl, K. Gronau, N. Pietack, M. Hecker, D. Becher, J. Stulke, The phosphoproteome of the minimal bacterium Mycoplasma pneumoniae: analysis of the complete known Ser/Thr kinome suggests the existence of novel kinases, Mol Cell Proteomics 9 (2010) 1228-1242. 10.1074/mcp.M900267-MCP200.

[27] D.J. Rigden, E. Lamani, L.V. Mello, J.E. Littlejohn, M.J. Jedrzejas, Insights into the catalytic mechanism of cofactor-independent phosphoglycerate mutase from X-ray crystallography, simulated dynamics and molecular modeling, J Mol Biol 328 (2003) 909-920. 10.1016/s0022-2836(03)00350-4.

[28] M.J. Jedrzejas, M. Chander, P. Setlow, G. Krishnasamy, Mechanism of catalysis of the cofactor-independent phosphoglycerate mutase from Bacillus stearothermophilus. Crystal structure of the complex with 2-phosphoglycerate, J Biol Chem 275 (2000) 23146-23153. 10.1074/jbc.M002544200.

[29] J. Delgado, L.G. Radusky, D. Cianferoni, L. Serrano, FoldX 5.0: working with RNA, small molecules and a new graphical interface, Bioinformatics 35 (2019) 4168-4169. 10.1093/bioinformatics/btz184.

[30] J. Schymkowitz, J. Borg, F. Stricher, R. Nys, F. Rousseau, L. Serrano, The FoldX web server: an online force field, Nucleic Acids Res 33 (2005) W382-388. 10.1093/nar/gki387.

[31] O. Trott, A.J. Olson, AutoDock Vina: improving the speed and accuracy of docking with a new scoring function, efficient optimization, and multithreading, J Comput Chem 31 (2010) 455-461. 10.1002/jcc.21334.

[32] A. Sajid, S. Lusvarghi, M. Murakami, E.E. Chufan, B. Abel, M.M. Gottesman, S.R. Durell, S.V. Ambudkar, Reversing the direction of drug transport mediated by the human multidrug transporter P-glycoprotein, Proc Natl Acad Sci U S A 117 (2020) 29609-29617. 10.1073/pnas.2016270117.

[33] G.M. Morris, R. Huey, W. Lindstrom, M.F. Sanner, R.K. Belew, D.S. Goodsell, A.J. Olson, AutoDock4 and AutoDockTools4: Automated docking with selective receptor flexibility, J Comput Chem 30 (2009) 2785-2791. 10.1002/jcc.21256.

[34] M.D. Hanwell, D.E. Curtis, D.C. Lonie, T. Vandermeersch, E. Zurek, G.R. Hutchison, Avogadro: an advanced semantic chemical editor, visualization, and analysis platform, J Cheminform 4 (2012) 17. 10.1186/1758-2946-4-17.

[35] J. Jimenez, M. Skalic, G. Martinez-Rosell, G. De Fabritiis, KDEEP: Protein-Ligand Absolute Binding Affinity Prediction via 3D-Convolutional Neural Networks, J Chem Inf Model 58 (2018) 287-296. 10.1021/acs.jcim.7b00650.

[36] H.C. Jubb, A.P. Higueruelo, B. Ochoa-Montano, W.R. Pitt, D.B. Ascher, T.L. Blundell, Arpeggio: A Web Server for Calculating and Visualising Interatomic Interactions in Protein Structures, J Mol Biol 429 (2017) 365-371. 10.1016/j.jmb.2016.12.004.

[37] C. Louis-Jeune, M.A. Andrade-Navarro, C. Perez-Iratxeta, Prediction of protein secondary structure from circular dichroism using theoretically derived spectra, Proteins 80 (2012) 374-381. 10.1002/prot.23188.

[38] K. Katoh, K. Misawa, K. Kuma, T. Miyata, MAFFT: a novel method for rapid multiple sequence alignment based on fast Fourier transform, Nucleic Acids Res 30 (2002) 3059-3066. 10.1093/nar/gkf436.

[39] H. Ashkenazy, S. Abadi, E. Martz, O. Chay, I. Mayrose, T. Pupko, N. Ben-Tal, ConSurf 2016: an improved methodology to estimate and visualize evolutionary conservation in macromolecules, Nucleic Acids Res 44 (2016) W344-350. 10.1093/nar/gkw408.

[40] E.A. Libby, S. Reuveni, J. Dworkin, Multisite phosphorylation drives phenotypic variation in (p)ppGpp synthetase-dependent antibiotic tolerance, Nat Commun 10 (2019) 5133. 10.1038/s41467-019-13127-z.

[41] M.B. Potters, B.T. Solow, K.M. Bischoff, D.E. Graham, B.H. Lower, R. Helm, P.J. Kennelly, Phosphoprotein with phosphoglycerate mutase activity from the archaeon Sulfolobus solfataricus, J Bacteriol 185 (2003) 2112-2121. 10.1128/JB.185.7.2112-2121.2003.

[42] T. Orthwein, J. Scholl, P. Spat, S. Lucius, M. Koch, B. Macek, M. Hagemann, K. Forchhammer, The novel PII-interactor PirC identifies phosphoglycerate mutase as key control point of carbon storage metabolism in cyanobacteria, Proc Natl Acad Sci U S A 118 (2021). 10.1073/pnas.2019988118.

[43] K. Watabe, E. Freese, Purification and properties of the manganese-dependent phosphoglycerate mutase of Bacillus subtilis, J Bacteriol 137 (1979) 773-778. 10.1128/jb.137.2.773-778.1979.

[44] R.P. Singh, P. Setlow, Purification and properties of phosphoglycerate phosphomutase from spores and cells of Bacillus megaterium, J Bacteriol 137 (1979) 1024-1027. 10.1128/jb.137.2.1024-1027.1979.

[45] N.J. Kuhn, B. Setlow, P. Setlow, Manganese(II) activation of 3-phosphoglycerate mutase of Bacillus megaterium: pH-sensitive interconversion of active and inactive forms, Arch Biochem Biophys 306 (1993) 342-349. 10.1006/abbi.1993.1521.

[46] A. Sharma, G. Chattopadhyay, P. Chopra, M. Bhasin, C. Thakur, S. Agarwal, S. Ahmed, N. Chandra, R. Varadarajan, R. Singh, VapC21 Toxin Contributes to Drug-Tolerance and Interacts With Non-cognate VapB32 Antitoxin in Mycobacterium tuberculosis, Front Microbiol 11 (2020) 2037. 10.3389/fmicb.2020.02037.

[47] R. Banerjee, G.G. Jayaraj, J.J. Peter, V. Kumar, K. Mapa, Monitoring conformational heterogeneity of the lid of DnaK substrate-binding domain during its chaperone cycle, FEBS J 283 (2016) 2853-2868. 10.1111/febs.13769.

[48] M. Sajish, S. Kalayil, S.K. Verma, V.K. Nandicoori, B. Prakash, The significance of EXDD and RXKD motif conservation in Rel proteins, J Biol Chem 284 (2009) 9115-9123. 10.1074/jbc.M807187200.

[49] J.T. Vivian, P.R. Callis, Mechanisms of tryptophan fluorescence shifts in proteins, Biophys J 80 (2001) 2093-2109. 10.1016/S0006-3495(01)76183-8.

[50] N. Dehghan-Nayeri, M. Rezaei tavirani, THE INTERPRETATION OF PROTEIN STRUCTURE THROUGH RELATIONSHIP OF MELTING POINT (TM) AND ENTHALPY OF UNFOLDING (ΔHU), 41 (2015) 2278-2246.

[51] I.B. Durowoju, K.S. Bhandal, J. Hu, B. Carpick, M. Kirkitadze, Differential Scanning Calorimetry - A Method for Assessing the Thermal Stability and Conformation of Protein Antigen, J Vis Exp (2017). 10.3791/55262.

[52] B. Xue, S. Leibler, Benefits of phenotypic plasticity for population growth in varying environments, Proc Natl Acad Sci U S A 115 (2018) 12745-12750. 10.1073/pnas.1813447115.

[53] M. Rescan, D. Grulois, E. Ortega-Aboud, L.M. Chevin, Phenotypic memory drives population growth and extinction risk in a noisy environment, Nat Ecol Evol 4 (2020) 193-201. 10.1038/s41559-019-1089-6.
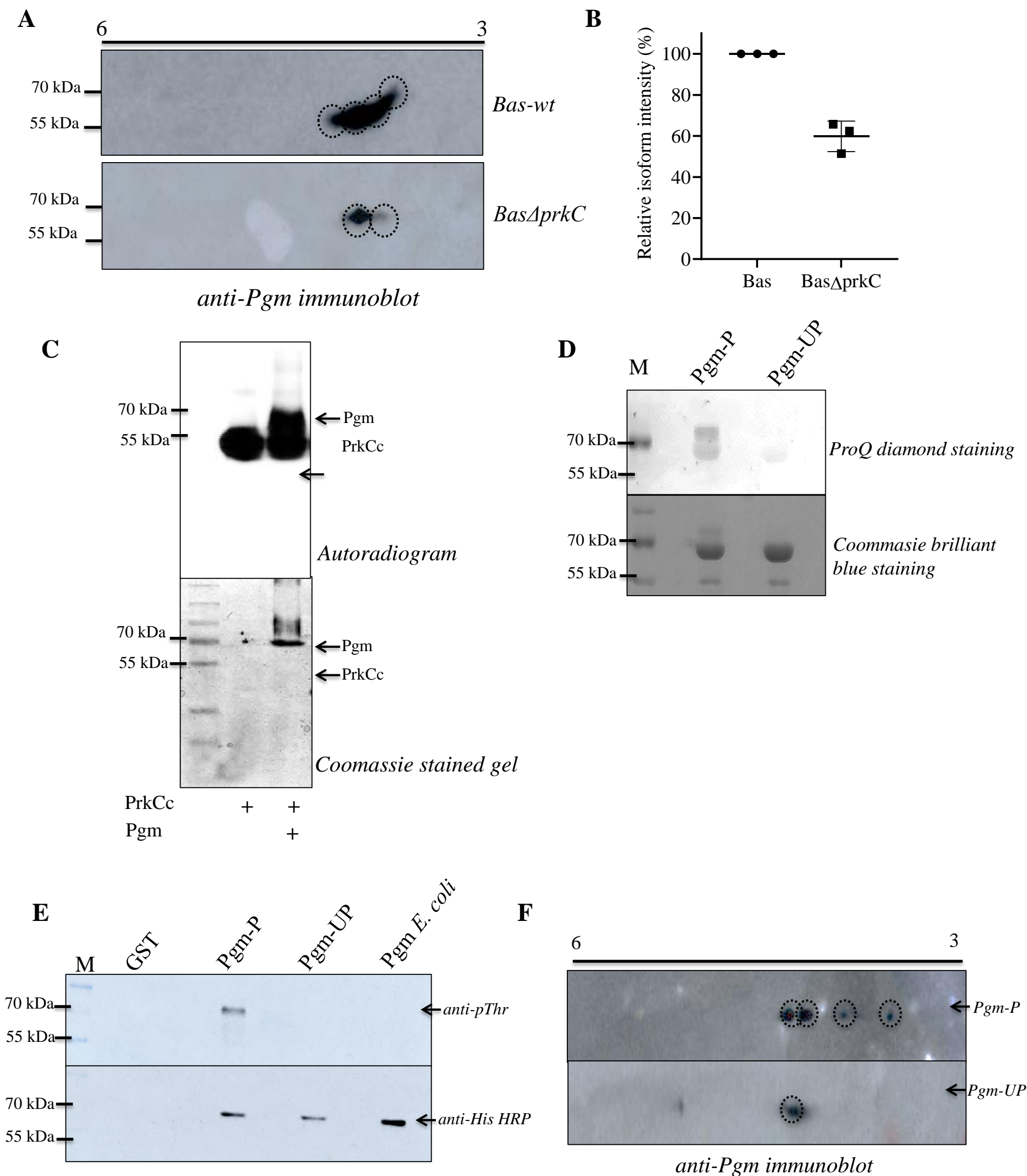
Figure 1. Pgm is phosphorylated by PrkC in *Bacillus anthracis*. (A) Whole cell lysates from Bas-wt and BasΔprkC were clarified and subjected to 2-D gel electrophoresis followed by immunoblotting using anti-Pgm antibodies. Multiple species of Pgm were observed in Bas-wt as compared to BasΔprkC and their relative intensities are calculated and plotted using GraphPad Prism (B). Bas-wt Phosphorylation was taken as 100%. The error bars showing S.D. of three independent experiments. (C) Autoradiogram showing Pgm (2 μg) phosphorylation by PrkC (0.5 μg) (upper panel). The corresponding SDS-PAGE is shown (lower panel). (D) Pgm-P and Pgm-UP were run on SDS-PAGE followed by ProQ diamond staining. The signal was analyzed using Typhoon imager (Upper panel). The proteins were stained by Coomasie brilliant blue for loading control (lower panel). (E) His-tagged Pgm purified from *E. coli* expressing PrkC (Pgm-P) and PrpC (Pgm-UP) was subjected to SDS-PAGE and probed with anti-pThr (upper panel) and anti-His HRP (lower panel). Pgm-P was found to be phosphorylated while there was no phosphorylation observed on Pgm-UP. (F) *E. coli* purified Pgm-P and Pgm-UP were subjected to 2-D gel electrophoresis followed by immunoblotting using anti-Pgm antibodies. Multiple species were observed in Pgm-P as compared to Pgm-UP confirming Pgm phosphorylation.

Figure 3

A

70 kDa —
55 kDa —
35 kDa —
←Pgm
←Eno
←PrkD
Autoradiogram

70 kDa —
55 kDa —
35 kDa —
Coomassie stained gel

PrkD	+	+	+
Eno	+		
Pgm		+	

B

←Pgm
←PrkG
←Eno
Autoradiogram

70 kDa —
55 kDa —
35 kDa —
Coomassie stained gel
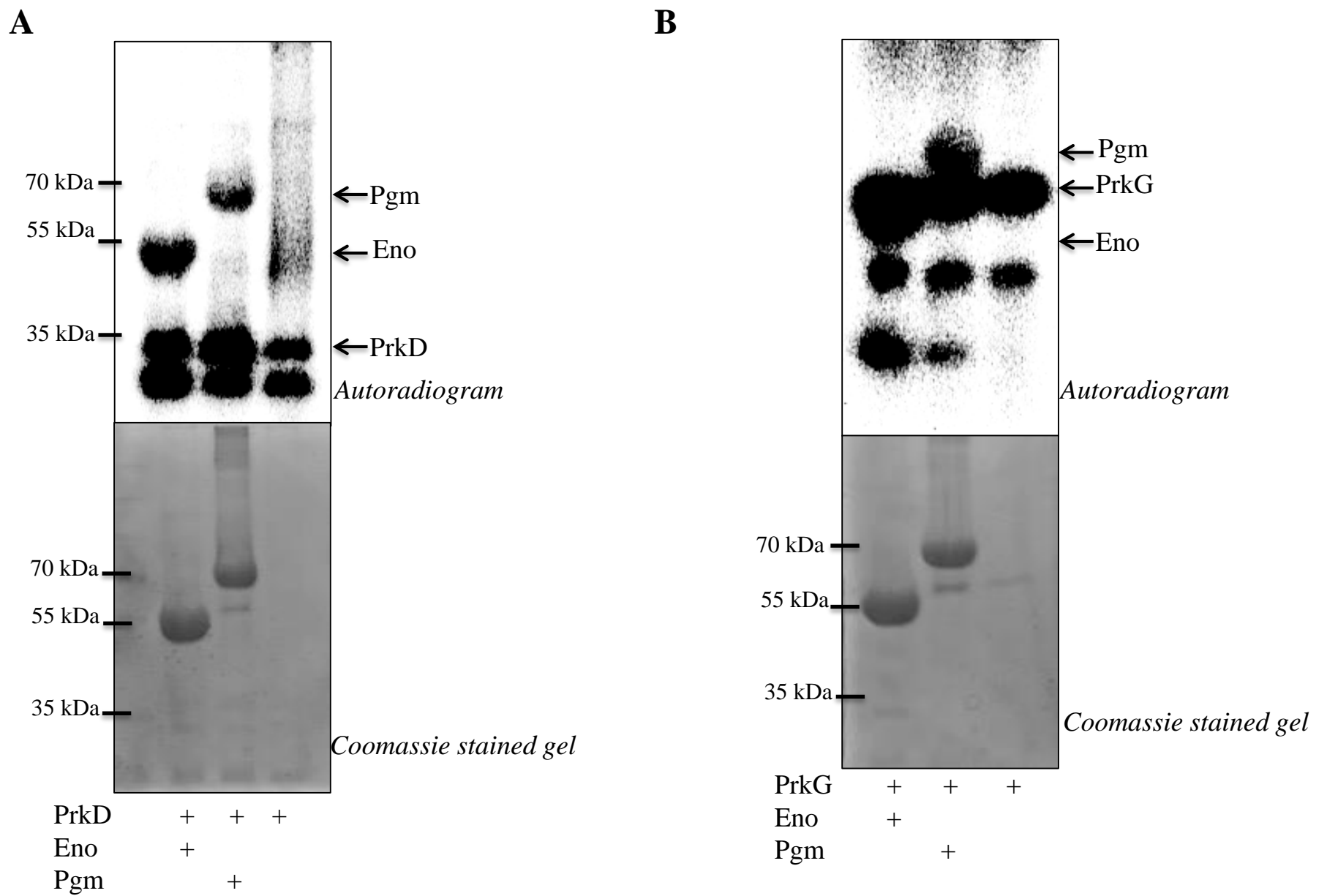
PrkG	+	+	+
Eno	+		
Pgm		+	

C
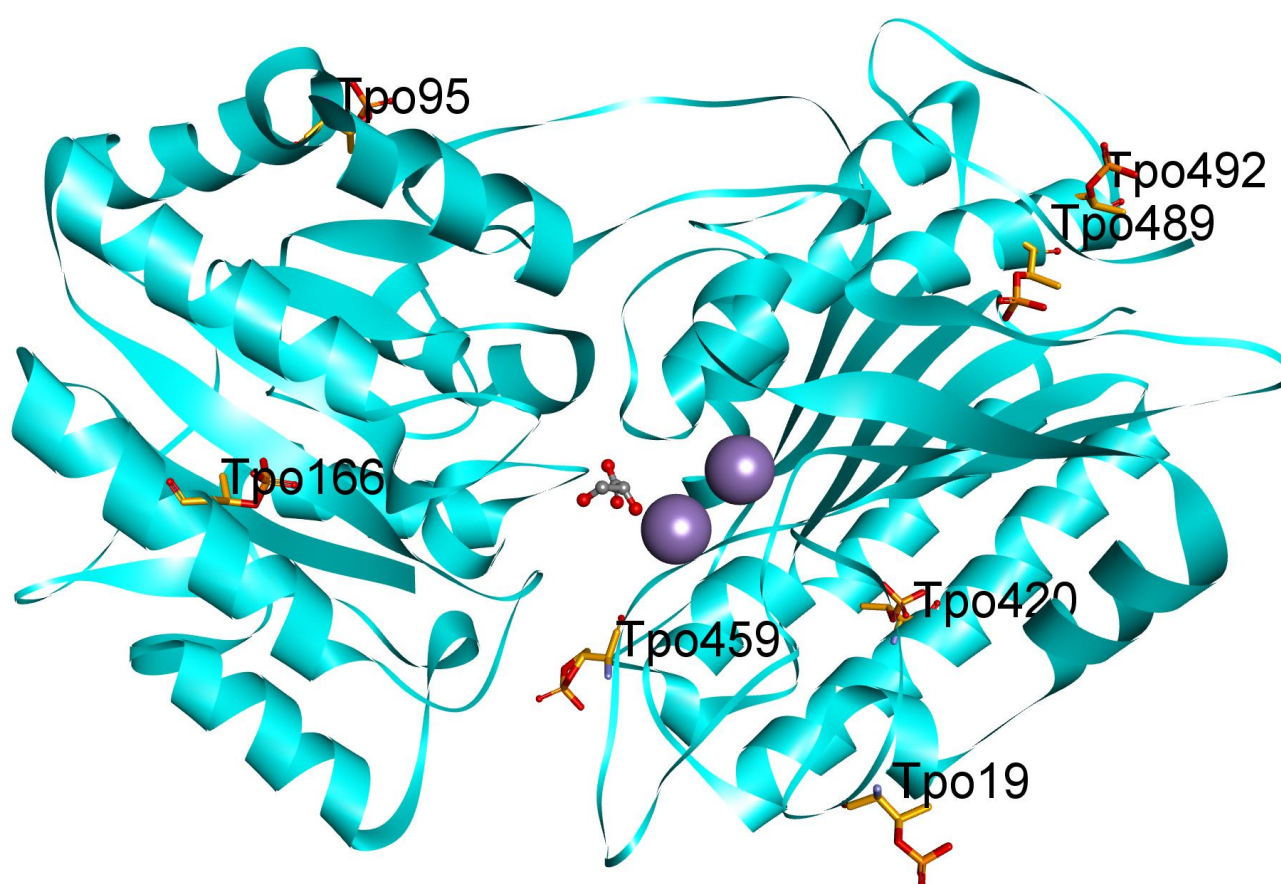
Figure 2. Pgm and Eno are phosphorylated by DSPK's PrkD and PrkG *in vitro*. (A and B) Autoradiogram (upper panel) showing phosphorylation of recombinant Pgm and Eno (5 μg) by PrkD (0.8 μg) **(A)** and PrkG (0.8 μg) **(B)** . The corresponding SDS-PAGE is shown (lower panel). **(C)** Mapping of phosphorylated residues on Pgm. Cartoon representation of Pgm-P structure depicts phosphorylation sites identified by mass spectrometry. Seven Thr residues (T19, T95, T166, T420, T459, T489 and T492) were identified and labeled above in the respective domains. Metal ions and phosphorylated amino acid residues, in blue and orange color respectively, represented by ball and stick model. (labeled as Tpo).

Figure 3

A
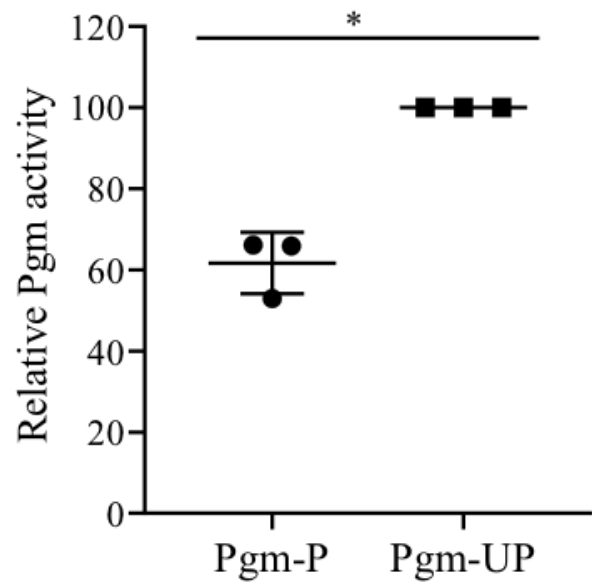
B
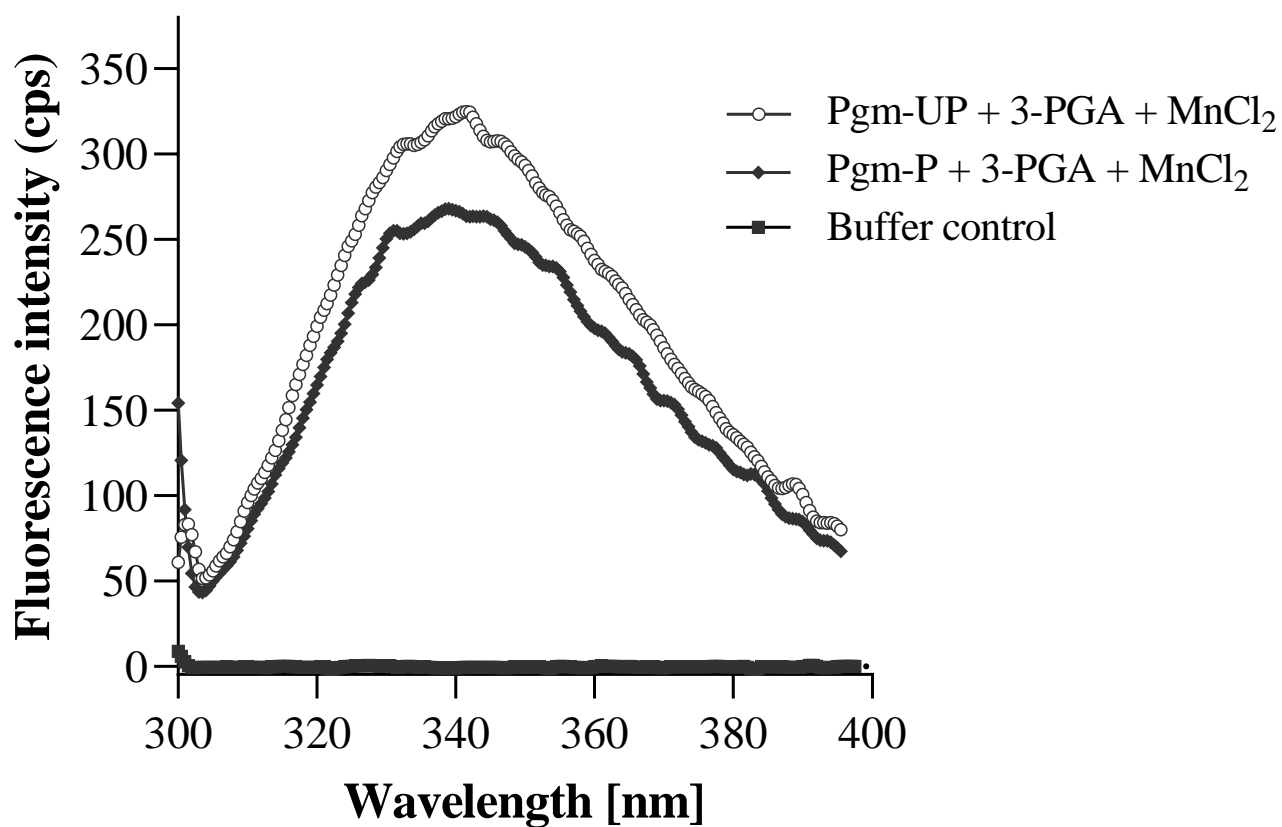
C
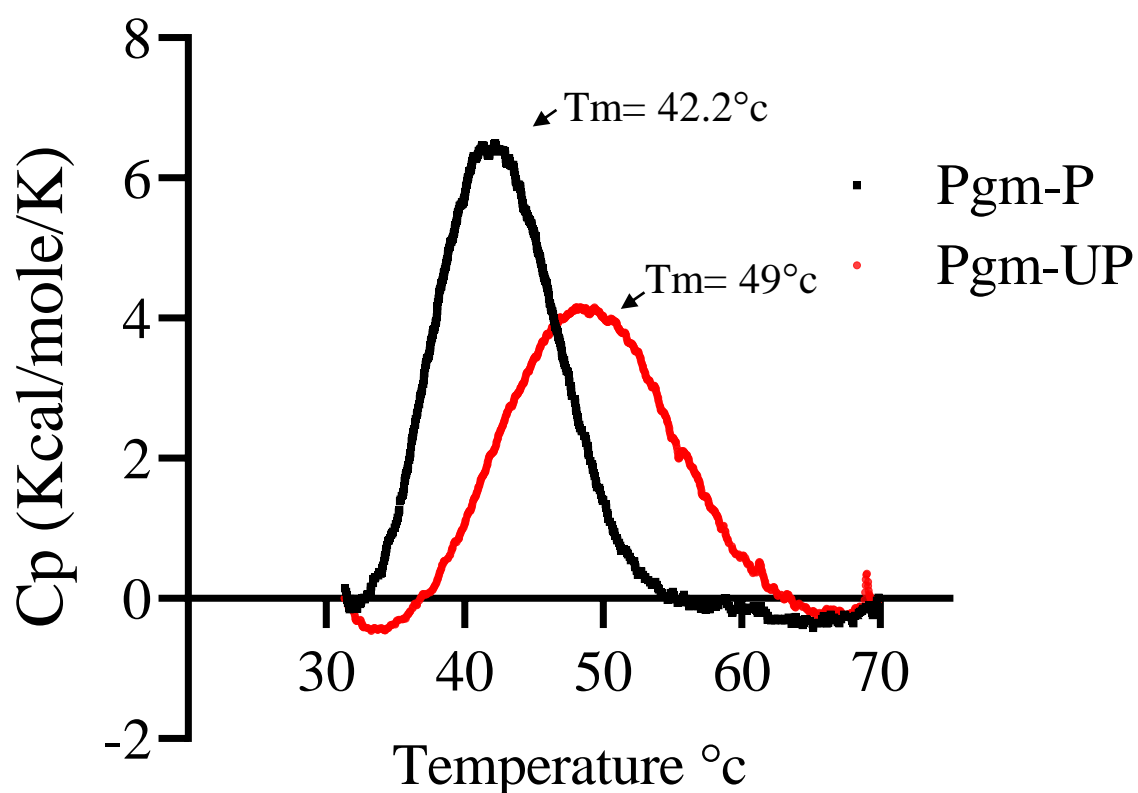
Figure 3. Effect of Phosphorylation on Pgm activity. (A) Graph showing relative activity of Pgm-P and Pgm-UP. The activity was calculated taking Pgm-UP as 100%. All experiments were performed thrice, and error bars represent SE of three independent values. *$P \leq 0.05$, **$P \leq 0.01$, ***$P \leq 0.001$, as determined by two-tailed unpaired Student's t test.**(B)** The interaction of Pgm-UP and Pgm-P (10 µM) with MnCl2 (0.5 M) was measured in terms of tryptophan fluorescence. The fluorescence was recorded from 330 nm to 430 nm after excitaton at 280 nm. Buffer alone was taken as control. **(C)** The enthalpy measurements of Pgm-P and Pgm-UP by Differential scanning calorimetry have been plotted with the Tm indication (by arrows).

Figure 4

A
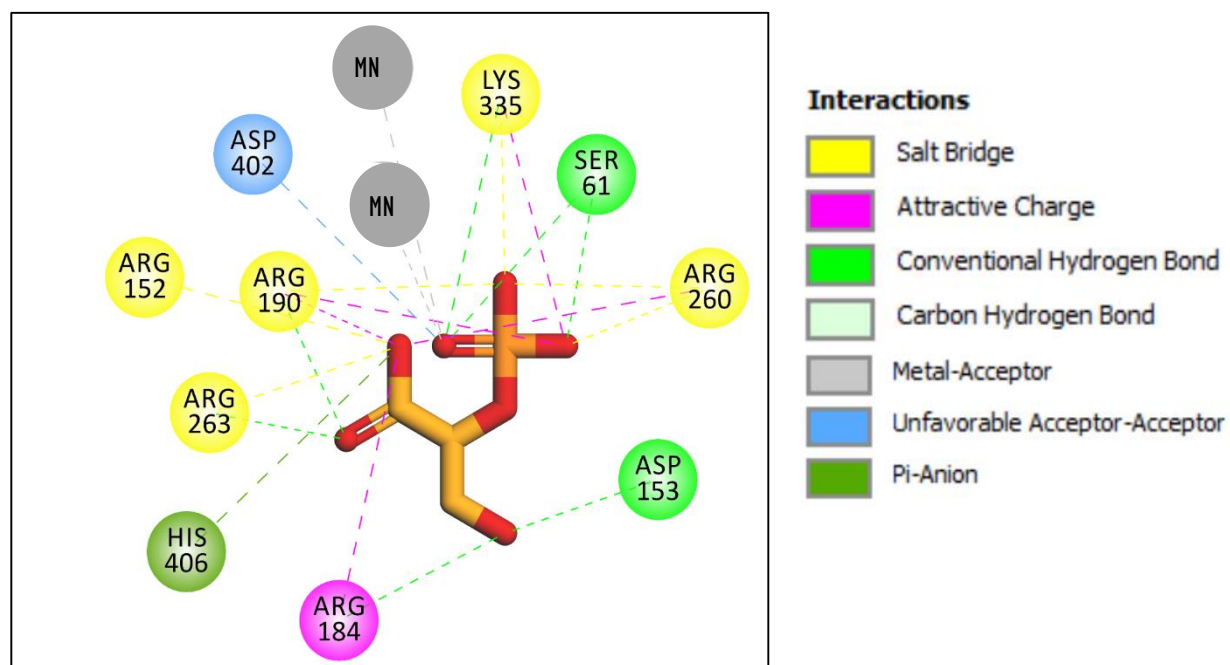
B
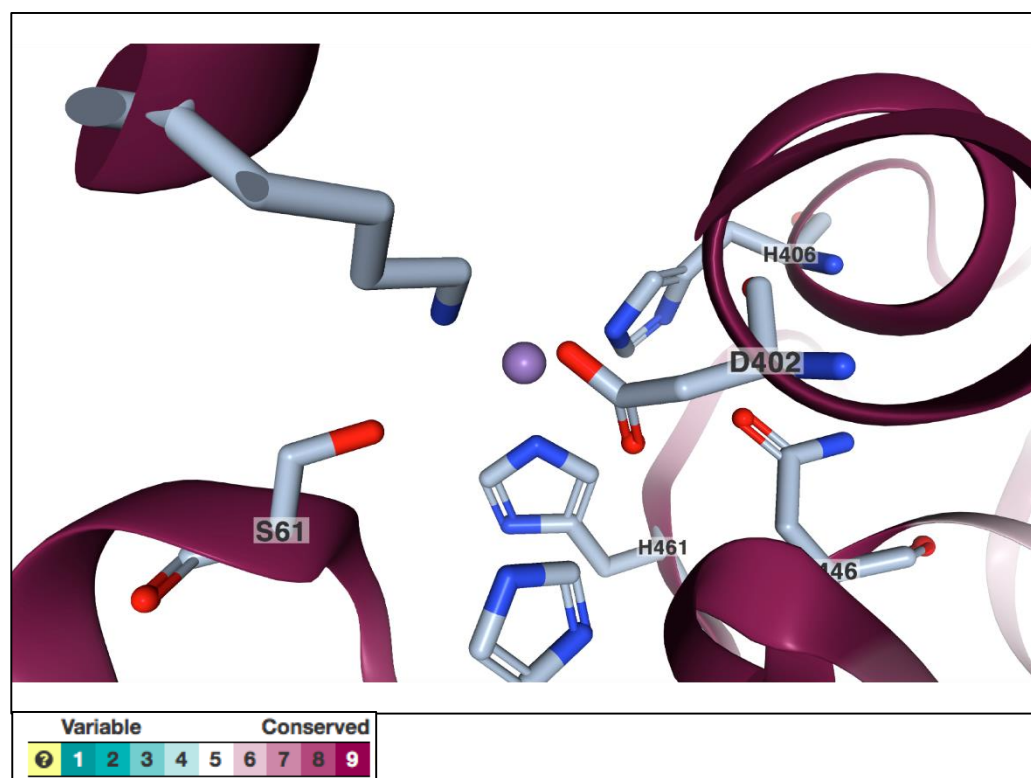
Figure 4. Pgm structure and domain conservation analysis. (A) 2D representation of Pgm-3-PGA interaction and the interacting residues. The residues are mapped on the homology model generated based on available Pgm structures (PDB: 2IFY, 1EJJ, 1EQJ, 1O98, 1O99). **(B) Cartoon representation of binding site:** The conservation of amino acids in Pgm is tested across 220 *Bacillus* sp. Ser61 and Thr459 (through His 461) are involved in metal ligand interaction and are found to be conserved across different *Bacillus* species. The color label for conservation level is depicted at the bottom.

# Figure 5

A

B
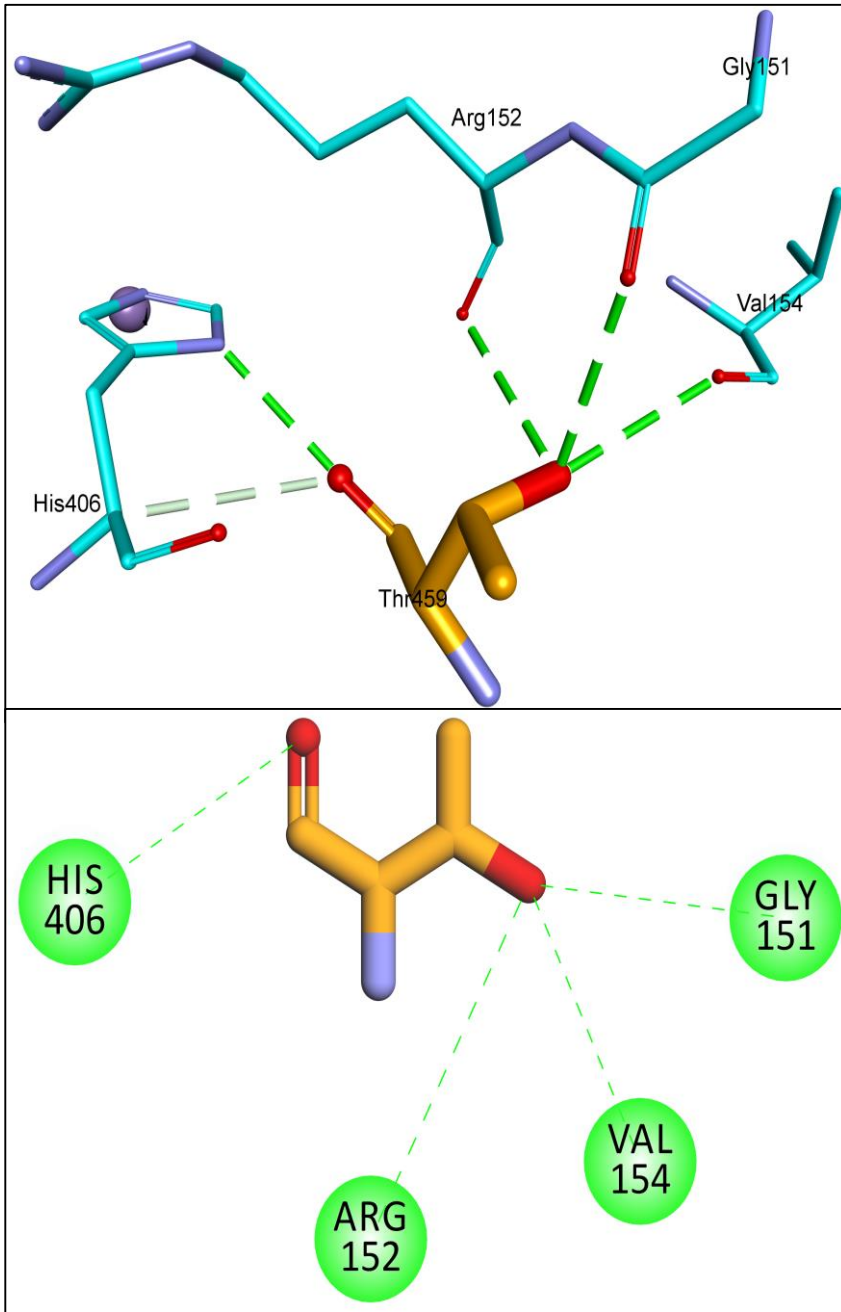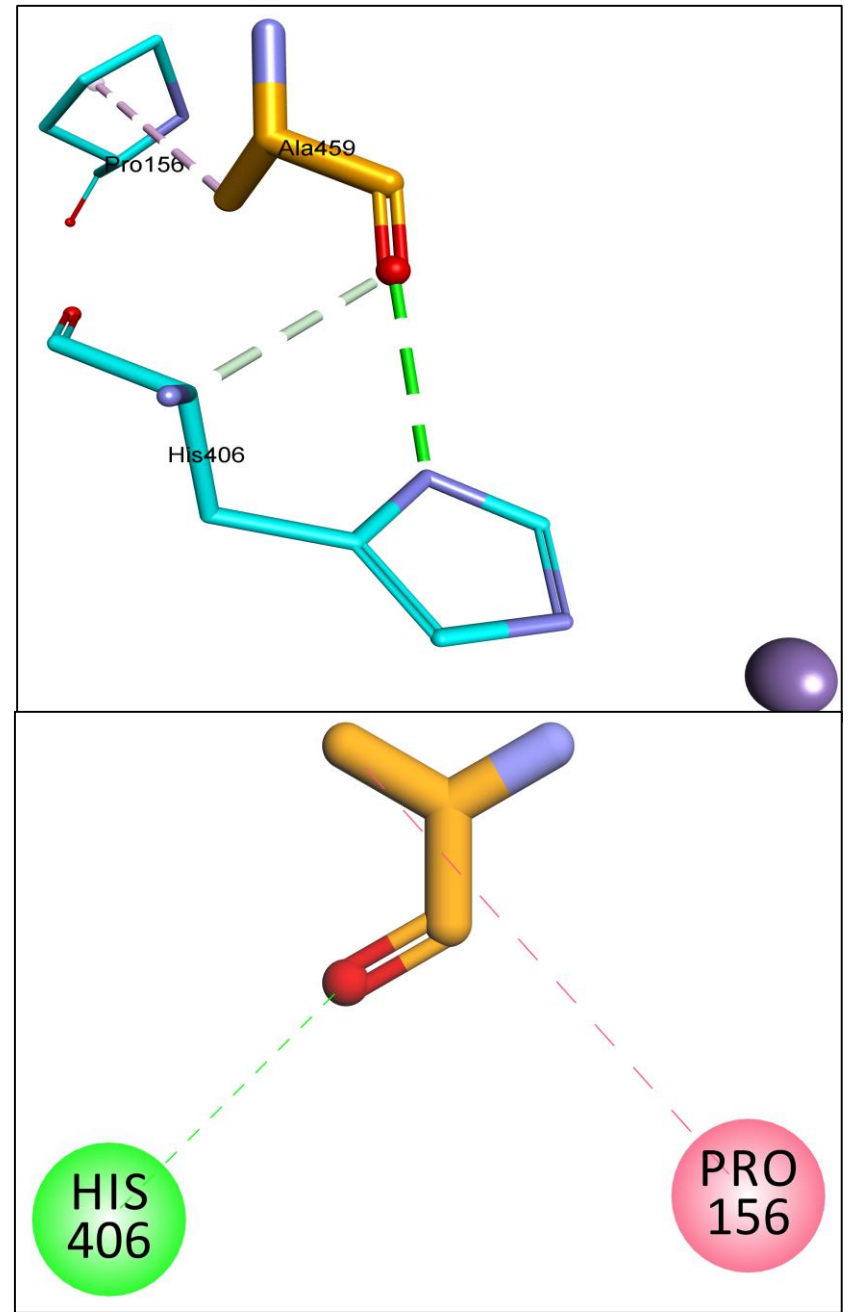
Pgm-WT

Pgm-T459A

Interactions

Conventional Hydrogen Bond

Carbon Hydrogen Bond

Alkyl

Figure 5. Comparative analysis of Thr459 interaction in wildtype (WT) and mutant (T459A) Pgm. Thr459 residue in the Pgm-WT develops stabilizing interactions with neighboring amino acid residues **(A)**. However, the Thr to Ala mutation of T459 residue disrupts most of the interactions potentially disrupting the hydrogen bonds with Arg152 which alters the domain cleft and conformation of the catalytic site **(B)**.

Click here to access/download
Supplementary Material (online publication only)
bbrc supplementary figures.pptx
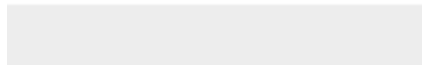
Declaration of interests

☒The authors declare that they have no known competing financial interests or personal relationships that could have appeared to influence the work reported in this paper.

☐The authors declare the following financial interests/personal relationships which may be considered as potential competing interests:

Gunjan Arora